Thermal Shock Behavior of a Three-Dimensional SiC/SiC Composite

SHOUJUN WU, LAIFEI CHENG, LITONG ZHANG, and YONGDONG XU

Thermal shock behavior of a three-dimensional (3-D) SiC/SiC composite was studied using the water-quenched method. Thermal shock damage of the composite was assessed by scanning electron microscopy characterization and residual three-point-bending strength. In the thermal shock process, the composite displayed the same bending mechanical behaviors as those of the original composite and retained 80 pct of the original strength in the longitudinal direction after being quenched from 1200 °C to 25 °C in water for 100 cycles. However, the composite displayed anisotropy in resistance to thermal shock damage. The observed microdamage processes were as follows: (1) formation of micropores and long crack, (2) transfer and growth of pores, (3) saturation of the dimension and the density of pores, and (4) accelerated growth of the long crack along the longitudinal direction. The critical thermal shock number for the composite was about 50. When thermal shock was less than 50 cycles, the residual flexural strength of the composite decreased with thermal shock cycles increasing. When the number was greater than 50, the strength of the composite did not decrease further.

I. INTRODUCTION

SILICON carbide fiber-reinforced SiC-matrix composites fabricated by the chemical vapor infiltration (CVI) process (SiC/SiC (CVI)) have been intensively researched as the most promising thermal structural materials.[1,2] Besides fundamental thermal and mechanical properties, thermal shock and thermal cycle effects are important factors limiting the performance of the composites for high-temperature application.

Thermal shock resistance of fiber-reinforced silicon carbide matrix composites has been the subject of increasing interest recently.[3–9] These studies have shown that the characteristics of thermal shock damage in fiber-reinforced composites were directly affected by the woven structure of the fiber preforms. Yin *et al.* studied the thermal shock behavior of a three-dimensional (3-D) C/SiC composite quenched in air.[4] The results indicated that there was a critical thermal shock cycle number of 50 cycles for 3-D woven C/SiC composite. When the cycles of thermal shocks were less than 50, the residual flexural strength of C/SiC composites decreased with the increase of the number. When the number of thermal shocks of C/SiC was greater than 50, the strength of C/SiC did not further decrease because the crack density was saturated. Kagawa documented the microdamage processes of a SiC/SiC composite consisting of a SiC matrix reinforced with a two-dimensional (2-D) SiC fiber fabric (Nicalon) fabricated by the CVI process.[8] Further, the observed microdamage processes of the composite were as follows: (1) microcracks initiated from the corners of pores; (2) crack growth between bundles and inside the bundles at the transverse plane; and (3) saturation of the crack density and formation of long cracks after three repeated thermal shock events. The surface of 2-D HI-NICALON* SiC/SiC composites under thermal shock indicates sublimation and trace melting.[9] However, the thermal shock behavior of HI-NICALON/SiC composites, especially those that are 3-D and quenched in water, has not been reported up to now.

In the present article, a 3-D HI-NICALON/SiC composite was prepared. Much of the analysis and discussion will then focus on the effects of thermal shock quenched in water on the evolution of microstructural damage, the flexural strength and the corresponding Young's modulus of the composite.

II. EXPERIMENTAL PROCEDURE

A. *Fabrication of the Specimens*

HI-NICALON silicon carbide fiber from Japan Nippon Carbon (Tokyo, Japan) was employed. The fiber preform was prepared using the four-step three-dimensional (4-step 3-D) braiding method and was supplied by the Nanjing Institute of Glass Fiber (Nanjing, People's Republic of China). The low-pressure chemical vapor infiltration (LPCVI) process was employed to deposit pyrolytic carbon interphase and the silicon carbide matrix. The volume fraction of fibers was about 40 pct and the braiding angle was about 20 deg. The scanning electron microscope (SEM) image of the 3-D composite preform fabricated by the 4-step 3-D braiding method is shown in Figure 1. The interfacial layer of pyrocarbon (PyC) was deposited for 10 hours at 870 °C and 5 kPa with C_3H_6. The deposited PyC interphase layer is about 0.2 μm. Methyltrichlorosilane (MTS, CH_3SiCl_3) was used for the deposition of the SiC matrix. The MTS vapor was carried by bubbling hydrogen. The conditions for deposition of SiC matrix were as follows: the deposition temperature was 1100 °C, the pressure was 5 kPa, the time was 120 hours, and the molar ratio of H_2 to MTS was 10. Argon was employed as the dilute gas to

*HI-NICALON is a trademark of Nippon Carbon Co., Tokyo, Japan.

SHOUJUN WU, Doctor, LAIFEI CHENG, LITONG ZHANG, and YONGDONG XU, Professors, are with the National Key Laboratory of Thermostructure Composite Materials, Northwestern Polytechnical University, Xi'an Shaanxi 710072, People's Republic of China. Contact e-mail: shoujun_wu@163.com

Manuscript submitted January 19, 2006.

slow the chemical reaction rate of deposition.[10] Specimens with the dimension of 2.4 mm in height, 4.3 mm in width, and 40.0 mm in length were machined from the as-received composites and polished. The density and open porosity of the as-received composite samples tested by Archimedes' technology were 2.67 $g \cdot cm^{-3}$ and 7.25 pct, respectively. A CVD SiC coating was prepared on the substrates for 20 hours to seal the open ends of the fibers after cutting from the prepared composite. The schematic of the specimen is shown in Figure 2.

B. *Thermal Shock Tests*

Thermal shock experiments were performed by quenching specimens from higher temperature in water for different cycles. The composite specimens were placed in an alumina (>99.8 pct) holder and heated in air in a $MoSi_2$ furnace at 1200 °C for 3 minutes to ensure the uniformity of temperature. The specimens were then quenched into a water bath at 25 °C for 2 minutes. The time elapsed between the opening of the furnace and the moment the specimens touched the water was approximately 5 seconds.

C. *Measurement of the Composites*

The residual flexural strength of the specimens was measured using the three-point-bending method, carried out on an Instron 1195 machine (Limited, Buckinghamshire, U.K.) at room temperature. The span dimension was 30 mm and the loading rate was 0.5 mm min^{-1}. The flexural strength σ was calculated by

$$\sigma = \frac{3}{2}\frac{P_{\max}L}{bh^2} \quad [1]$$

where L, b, and h are the span, thickness, and height of the specimens, respectively. The term $P_{\max}$ is the maximum flexural load during the test.

Morphologies of the specimens before and after thermal shock tests were observed using a S4700 SEM.

III. RESULTS AND DISCUSSION

Figure 3 shows the relationship between the thermal shock cycles, N, and the residual strength of the 3-D SiC/SiC composite. As shown in Figure 3, with the increase of thermal shock cycles, the residual flexural strength of the composite decreased gradually. When $n > 50$, however, the strength did not decrease further until N was as high as 100 cycles. After the composite was quenched for 100 cycles, the residual flexural strength in the longitudinal direction was still retained 80 pct of the original value. Figure 4 shows typical bending load-displacement curves of the 3-D SiC/SiC composite after thermal shock for different cycles.

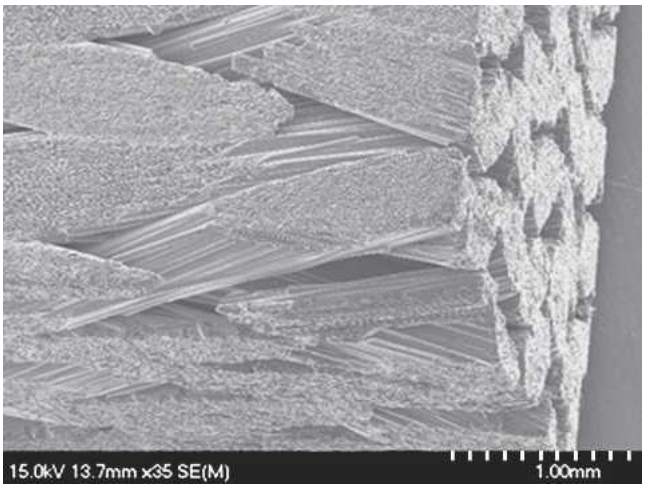

Fig. 1—SEM image of the 3-D composite preform fabricated by the 4-step 3-D braiding method.

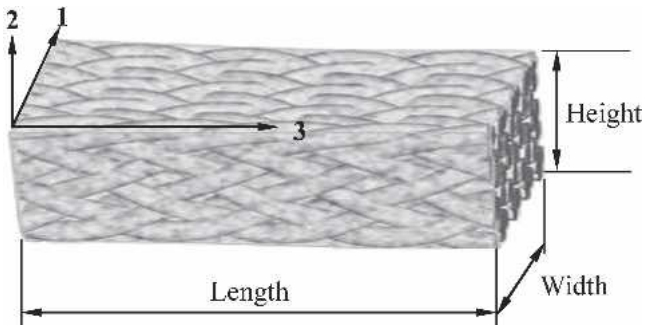

Fig. 2—Schematic of the specimen.

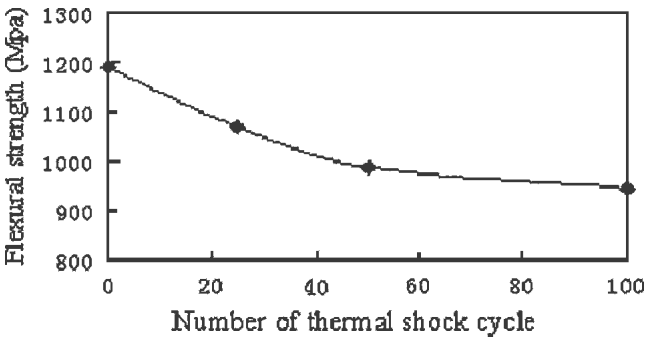

Fig. 3—Relations between the number of thermal shock cycles and residual strength of the 3-D SiC/SiC composite.

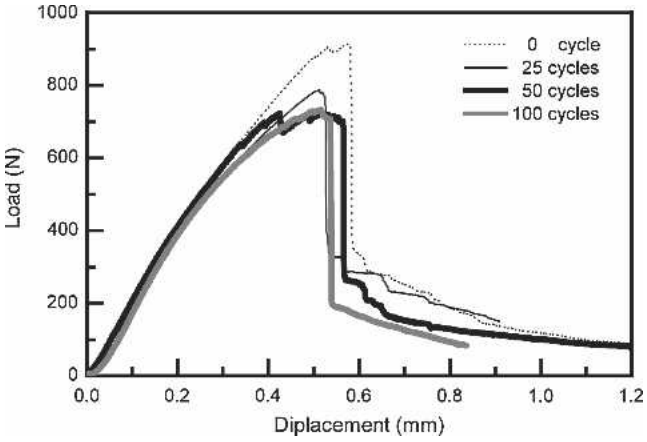

Fig. 4—Typical bending load-displacement curves of SiC/SiC composite after thermal shock for different cycles.

As shown in Figure 4, the bending mechanical behaviors of the quenched composite were similar to that of the original composite and had nearly the same value of corresponding Young's modulus. The flexural mechanical properties of the 3-D SiC/SiC composite before and after tests were shown in Table I.

In general, Young's modulus data are more representative to the overall damage state of the material than destructive strength test data because those changes induced by crack formation reflect the entire crack population, whereas the strength changes are related to changes in the critical flaw length only.[11] The preceding results indicated that the composite had excellent thermal shock resistance in the longitudinal direction.

Figure 5 shows the top surface micromorphologies of specimens after thermal shock. As shown in Figure 4, micropores and a long crack were produced in the coating during the thermal shock process. With the increase in the cycles of thermal shock, N, the dimension of micropores and the width of the long thermal shock crack produced in coating increased, while the number of the micropores decreased. The dimension and density of micropores were saturated after 50 cycles, while the crack width was enlarged. When quenched for 100 cycles, the corresponding crack width approached about 56 μm, which was much larger than 12.5 and 18 μm, corresponding to 25 and 50 cycles, respectively. According to the evolution of the micromorphologies of the shock damage, the shock damage processes of the composite were as follows: (1) formation of micropores and long crack, (2) transfer and growth of the pores, and (3) saturation of the dimension and the density of pores and accelerated growth of the long crack in width after $n > 50$.

Figure 6 shows interior micromorphologies of the geometrical neutral plane (plane (1,3)) in the height direction, which is parallel to the longitudinal direction. No crack or micropore was observed at $n < 50$, yet the fact that the long thermal shock crack penetrated into the interior of the composite is significant at $n = 100$. These shock damage characters of 3-D SiC/SiC were obviously different from those of 3-D C/SiC, demonstrated by Yin *et al.*[4] From the cross-sectional micromorphology of the specimen after 100 cycles thermal shock in Figure 7, it can be seen that the specimen cracked through the width at $n = 100$.

Table I. Flexural Mechanical Properties of the 3-D SiC/SiC Composite before and after Tests

Specimens State	As Received	Oxidized at 1200 °C in Air for 15 h	Thermal Shock		
			25 cycles	50 cycles	100 cycles
Residual flexural strength (MPa)	1193	1283	1071	988	945
Young's modulus (GPa)	230	201	223	221	218

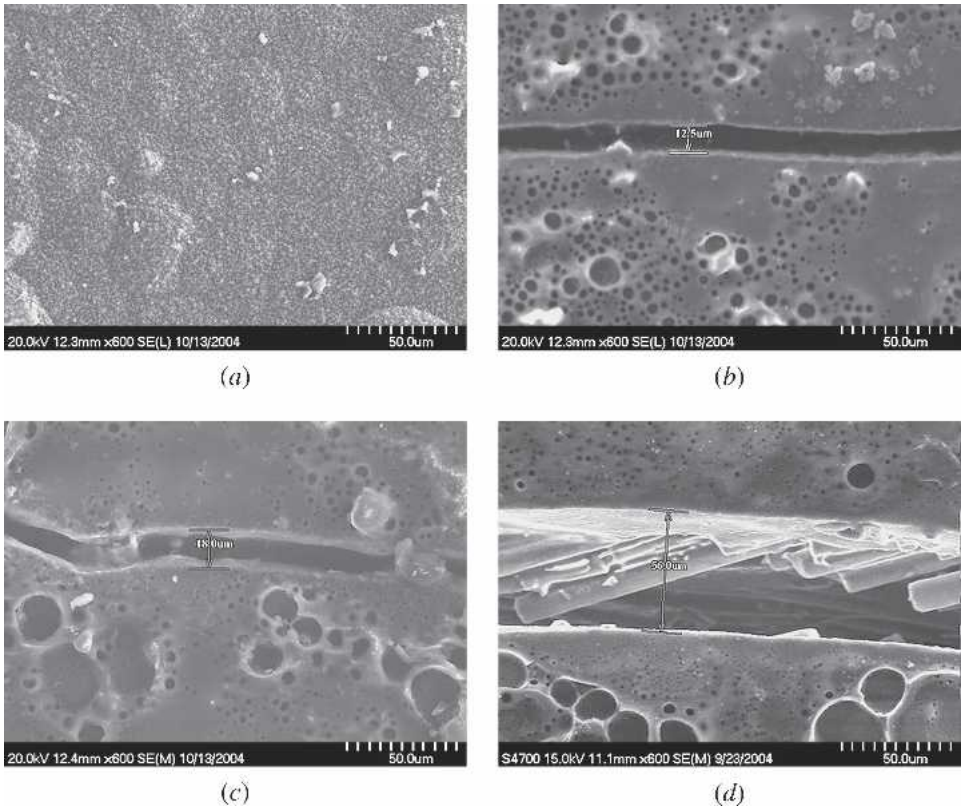

Fig. 5—Top surface micromorphologies after thermal shock for (*a*) 0 cycles, (*b*) 25 cycles, (*c*) 50 cycles, and (*d*) 100 cycles.

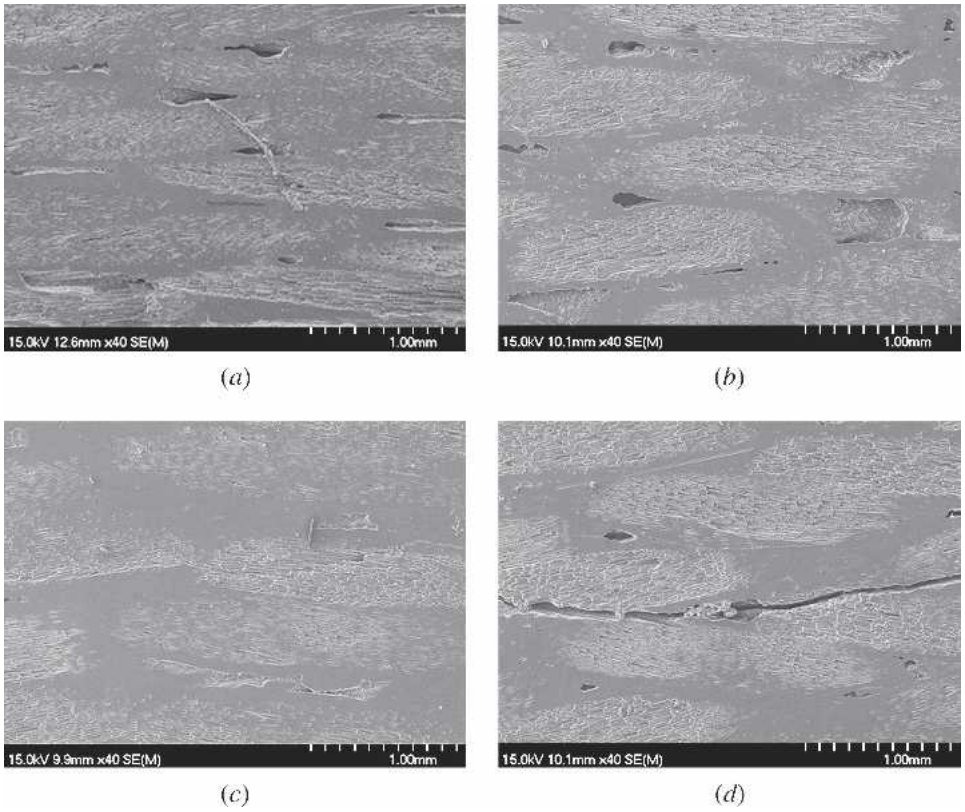

Fig. 6—Interior micromorphologies of thermal shock damage in the geometrical neutral plane (1,3): (*a*) 0 cycles, (*b*) 25 cycles, (*c*) 50 cycles, and (*d*) 100 cycles.

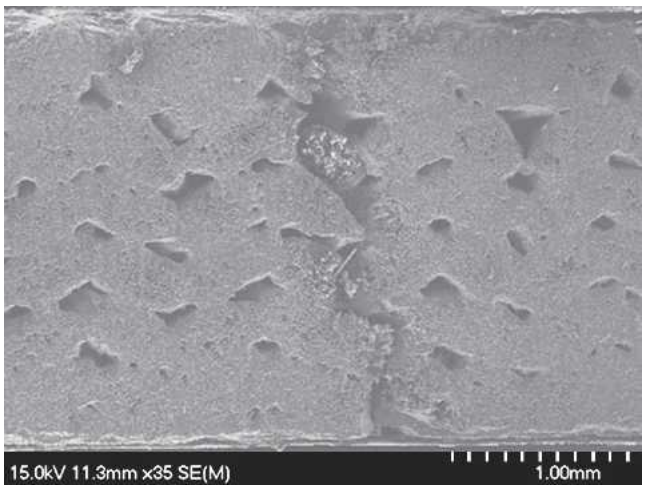

Fig. 7—Cross-sectional morphology after 100 cycles thermal shock.

In this work, the samples were put in air at 1200 °C for 3 minutes in each cycle. For 100 cycles, the total oxidation time in air will be 300 minutes (5 hours). Therefore, silica was produced by the oxidation of SiC. In fact, there was SiO_2 film produced on the surface of SiC coating due to oxidation, as shown in Figure 8. The thickness of SiO_2 film would increase with the increase of oxidation time (thermal shock cycles). Wet oxidation behaviors of SiC have shown that the silica will be volatilized by $Si(OH)_4$ and result in bubbles or pores produced due to the bubbles breaking.[11,12,13] When specimens at high temperature touched the cold water, the CVD SiC coating on the specimens' surfaces underwent wet oxidation. Hence, micropores were produced in the silica on the specimens' surface and their number and dimension increased as thermal shock cycles increased. Though the pores can affect the mechanical properties of the composite,[14] the oxidation mainly took place on the specimens' surfaces, and the strength degradation resulting from oxidation was very small. From Table I, it was clear that even after oxidization at 1200 °C for 15 hours, there was no strength degradation. Hence, the strength degradation of the composite in the thermal shock resulting from oxidation was very small. During the rapid cooling process in thermal shock, a large temperature difference was produced between the inside and surface of the composite. Under this temperature difference, the surface of the specimens endures tensile stress while the inner of the specimens endures compressive stress. Thus, crack would be produced on the materials' surfaces and extended as thermal shock cycles increased.

For composite, when the temperature difference reaches a critical value (ΔT_c), the induced thermal stress (σ_{TS}), sufficient to generate cracks in the matrix, is directly related to the difference in the thermal expansion coefficient (CTE) between the fiber and matrix.[15] For the C/SiC composite, the T300 carbon fiber is an anisotropic material and is characterized by two CTEs: a longitudinal CTE of -0.1 to -1.1×10^{-6}/°C and a radial CTE of 7.0×10^{-6}/°C.[16,17] The CTE of SiC matrix is about 4.6×10^{-6}/°C.[18] Hence,

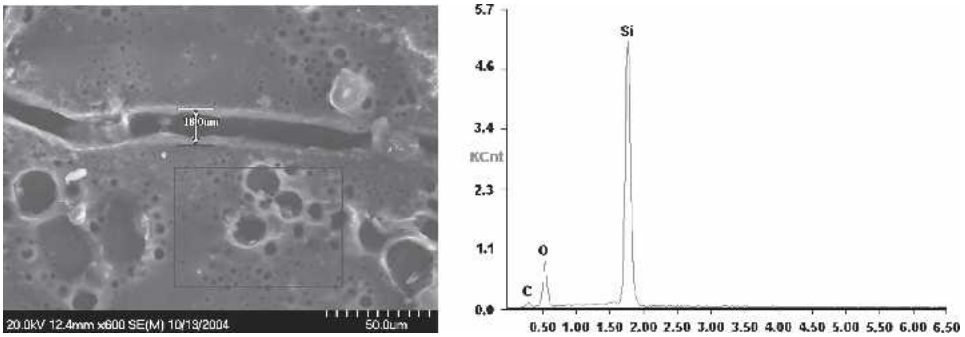

Fig. 8—Energy-dispersive spectrum of the specimen after 50 cycles thermal shock.

the matrix encounters tensile stress during the cooling process and microcracks will be produced in the SiC matrix perpendicular to the carbon fiber axis. For the SiC/SiC composite, the CTE of HI-NICALON SiC fiber is 3.1 to 3.5×10^{-6}/°C.[1,19] Thus, less tensile stress is produced in the matrix during the cooling process, which is much lower than that in the C/SiC composite, and the thermal cracks are scarcely produced in the SiC matrix. However, during the heating process, the expansion of the matrix is larger than that of HI-NICALON fiber. Thus, the matrix undergoes compressive stress under the constraint of the fibers, while the HI-NICALON fiber undergoes tensile stress, which will result in fiber break. Then, the matrix around the break fibers will encounter tensile stress in the subsequent thermal shock and gradually crack with increasing thermal shock cycles, as shown in Figure 5(d).

All of the preceding results indicated that the thermal shock damage of the composite was anisotropic. Resistance to thermal shock damage in the width direction was inferior to that in the height and the length directions. For 4-step 3-D braided composite, the mechanic properties are also anisotropic.[20] The strength in longitudinal direction is higher than that in transversal direction. Consequently, the anisotropy in thermal shock resistance of the composite might be the result of its braid structure.

The results also indicated that there was a critical value for the quench cycles of SiC/SiC composite. The residual flexural strength of the composite decreased with the thermal shock cycles increase when the times were below the critical value. When the quench number reached the critical value, the residual flexural strength of the composite did not decrease further with the increase of thermal shock cycles.

In the present experiment, the critical number of quench cycles was about 50. With the increase of quench cycles during the initial stage of thermal shock, stress concentration, which occurred at the corners of the pores, was reduced by the release of strain energy due to the micropore growth. The spread of most micropores emerging from the pores stopped when the tip of one micropore reached another pore, which might cause the formation of a long crack and successive decrease of strength. Above the critical value, the density of micropores would saturate. Then, some micropores linked together to form a long crack, which resulted in the composite rupture in the weak direction and the stress reduction. Therefore, the strength of the composite did not decrease further.

IV. CONCLUSIONS

1. In the thermal shock process, the 3-D SiC/SiC composite displayed the same bending mechanical behavior and values of the Young's modulus as those of the original composite, and retained 80 pct of the original strength in the longitudinal direction after quenching from 1200 °C to 25 °C in water for 100 cycles. However, the composite displayed anisotropy in resistance to thermal shock damage. The resistance to thermal shock damage in the width direction is inferior to those of other directions.
2. The observed microdamage processes of the composites were as follows: (1) formation of micropores and long crack, (2) transfer and growth of the pores, (3) saturation of the dimension and the density of pores and accelerated growth of the long crack in width after $n > 50$.
3. The critical number of thermal shock for the SiC/SiC composite was about 50 cycles. When the number was less than 50 cycles, the residual flexural strength of the SiC/SiC composite decreased with the increase of thermal shock cycles, while the Young's module retained was nearly the same as those of the original specimens. When the cycles of thermal shock of SiC/SiC were greater than 50, the strength of the SiC/SiC composite did not decrease further because the density of micropores was saturated, while the module decreased greatly.

ACKNOWLEDGMENTS

The authors acknowledge the support of the Chinese National Foundation for Natural Sciences under Contract No. 90405015 and the NSFC Distinguished Young Scholars under Contract No. 50425208, 2004.

REFERENCES

1. R. Naslain: *Compos. Sci. Technol.*, 2004, vol. 64, pp. 155-70.
2. J. Kimmel, N. Miriyala, J. Price, K. More, P. Tortorelli, H. Eaton, G. Linsey, and E. Sun: *J. Eur. Ceram. Soc.*, 2002, vol. 22, pp. 2769-75.
3. H. Wang and R.N. Singh: *J. Am. Ceram. Soc.*, 1996, vol. 79, pp. 1783-92.
4. X.W. Yin, L.F. Cheng, L.T. Zhang, and Y.D. Xu: *Carbon*, 2002, vol. 40, pp. 905-10.
5. N. Chawla, K.K. Chawla, M. Koopman, B. Patel, C. Coffin, and J.I. Eldridge: *Compos. Sci. Technol.*, 2001, vol. 61, pp. 1923-30.
6. K. Park and T. Vasilos: *Scripta Mater.*, 1998, vol. 39, pp. 1593-98.

7. K. Fujii and R. Yamada: *J. Nucl. Mater.*, 1998, vol. 258-263, pp. 1953-59.
8. Y. Kagawa: *Compos. Sci. Technol.*, 1997, vol. 51, pp. 607-11.
9. J. Yu, Z.W. Yao, G. Yu, F.M. Chu, X.Z. Tang, Y. Zeng, and T. Noda: *J. Nucl. Mater.*, 2000, vols. 283–287, pp. 1077-80.
10. Y.D. Xu, L.F. Cheng, L.T. Zhang, X.W. Yin, and H.F. Yin: *Ceram. Int.*, 2001, vol. 27, pp. 565-70.
11. E.J. Opila: *J. Am. Ceram. Soc.*, 2003, vol. 86, pp. 1238-48.
12. M. Maeda, K. Nakamura, and T. Ohkubo: *J. Mater. Sci.*, 1998, vol. 23, pp. 3933-38.
13. E.J. Opila: *J. Am. Ceram. Soc.*, 1994, vol. 77, pp. 730-36.
14. R.A. Dorey, J.A. Yeomans, and P.A. Smith: *J. Eur. Ceram. Soc.*, 2002, vol. 22, pp. 403-09.
15. A.R. Boccaccini: *Scripta Mater.*, 1998, vol. 38, pp. 1211-17.
16. http://www.torayusa.com/cfa/product.html.
17. Y.D. Xu, L.F. Cheng, L.T. Zhang, H.F. Yin, and W.C. Zhou: *J. Mater. Sci.*, 1999, vol. 34, pp. 6009-14.
18. W. Yang, A. Kohyama, T. Noda, Y. Katoh, T. Hinoki, H. Araki, and J. Yu: *J. Nucl. Mater.*, 2002, vols. 307–311, pp. 1088-92.
19. H. Ichikawa: *Ann. Chim.- Sci. Mater.*, 2000, vol. 25, pp. 523-28.
20. X.K. Sun and C.J. Sun: *Compos. Struct.*, 2004, vol. 65, pp. 485-92.